

Article

# A Study on the Bond Strength of Plastic–Metal Direct Bonds Using Friction Press Joining

Stefan P. Meyer <sup>\*</sup>, Maren T. Herold, Jan B. Habedank and Michael F. Zaeh

Institute for Machine Tools and Industrial Management, Technical University of Munich, Boltzmannstr., 15, 85748 Garching, Germany; Maren.herold@tum.de (M.T.H.); Jan.Habedank@iwb.tum.de (J.B.H.); Michael.zaeh@iwb.tum.de (M.F.Z.)

\* Correspondence: stefan.meyer@iwb.tum.de; Tel.: +49-(0)89-289-15548

**Abstract:** Friction press joining (FPJ) is an innovative joining process for bonding plastic components and metal sheets without additives in an overlap configuration. This paper focuses on the resulting bond strength. Tensile tests showed that the direct bonds produced by FPJ have either an equivalent or a higher bond strength compared to adhesive bonds. For the material combination of HD-PE and EN AW-6082-T6, an equivalent bond strength was achieved. In contrast, for the material combinations PA6-GF30 with EN AW-6082-T6 and PPS-CF with EN AW-2024-T3, higher tensile shear strengths were achieved via the FPJ technology. In addition to the technical considerations, this paper presents an evaluation of the technological maturity of FPJ. It was found that the basics of the technology are already well developed, and prototypes for showing the applicability have already been manufactured. The last part of this paper deals with the classification of FPJ into the standard for manufacturing processes, according to DIN 8593. The authors suggest a categorization into Activation bonding (item 4.8.1.3). These investigations show the high technical potential of FPJ for joining plastic components with metals.

**Keywords:** friction press joining; polymer metal joining; hybrid bonds; adhesive bonding; benchmark study; friction lap welding; technology readiness level



**Citation:** Meyer, S.P.; Herold, M.T.; Habedank, J.B.; Zaeh, M.F. A Study on the Bond Strength of Plastic–Metal Direct Bonds Using Friction Press Joining. *Metals* **2021**, *11*, 660. <https://doi.org/10.3390/met11040660>

Academic Editor: Francesco Lambiase, António Bastos Pereira and Leszek Adam Dobrzanski

Received: 14 March 2021  
Accepted: 15 April 2021  
Published: 18 April 2021

**Publisher's Note:** MDPI stays neutral with regard to jurisdictional claims in published maps and institutional affiliations.



**Copyright:** © 2021 by the authors. Licensee MDPI, Basel, Switzerland. This article is an open access article distributed under the terms and conditions of the Creative Commons Attribution (CC BY) license (<https://creativecommons.org/licenses/by/4.0/>).

## 1. Introduction

Modern aircraft consist of more than 50 wt% of (fiber-reinforced) plastics [1]. However, aluminum alloys are also used, particularly in the wing and the body structures. As a result, these two material types have to be joined at many interfaces. Thus far, adhesive bonding is state of the art in aerospace joining technology [2].

Nonetheless, adhesive bonding entails several disadvantages, such as the curing time and the additional mass introduction through the adhesive itself. One method to avoid these is direct joining. Direct joining is a very challenging but a desirable process for plastic–metal composites and is used in particular in different manufacturing sectors such as the tape-laying process for additive manufacturing [3], injection molding [4,5], ultrasonic welding [6] and thermal joining [7].

Another highly promising process among the direct joining technologies is friction press joining (FPJ), which is used to join semi-finished products (metal sheets and plastic components) [8]. To enable the transfer of this technology from the research level to an industrial application, it is essential to analyze the technological and economic potential. For this reason, this paper deals with the comparison of the bond strengths, the technological readiness and the technological potential of FPJ with structural adhesive bonding. Finally, recommendations for further developments of the FPJ technology are derived.

## 2. State of the Art

### 2.1. Friction Press Joining

Friction press joining is a novel joining process for the direct bonding of plastic components and metals, as studied by Wirth et al. [9]. Direct joining (or direct bonding) is defined as joining two parts without using additional material (e.g., adhesives, rivets or screws).

According to Meyer et al. [8], the process of FPJ is divided into five steps, analogously to friction stir welding (FSW). The first step—the surface pretreatment—is an upstream process that significantly influences the bond strength between the joining partners [8]. The actual joining process consists of a sequence of four individual actions (see Figure 1):

0. **Surface modification:** In this preliminary process step, the joining zone of the metallic joining partner is pretreated to increase the cohesive forces in the bond.
1. **Touch-down:** In the first phase of the joining process, a cylindrical tool rotates (rotational speed  $n$ ) around its longitudinal axis. By applying an axial force  $F_a$ , the tool presses onto the metallic surface in the negative  $z$ -direction. This plunging phase ends when the tool has reached a certain  $z$ -position, or a specified axial force is applied.
2. **Dwelling:** The tool remains at the plunge spot for a defined time  $t_V$ . This dwelling causes a heating and subsequent deformation of the material, resulting in the release of dissipative energy and a further heating of the process zone.
3. **Joining:** The tool is guided with a constant feed rate  $v$  along the metallic joining partner's surface. The plastic melts in the joining zone, which results in a bonding to the pretreated joining surface (after cooling). (Previous publications referred to Phase 3 as welding. In this paper, we use the term *joining* and explain the reasons for this rephrasing in Section 6.)
4. **Retreat:** The joining process ends with the retraction of the tool in the positive  $z$ -direction.

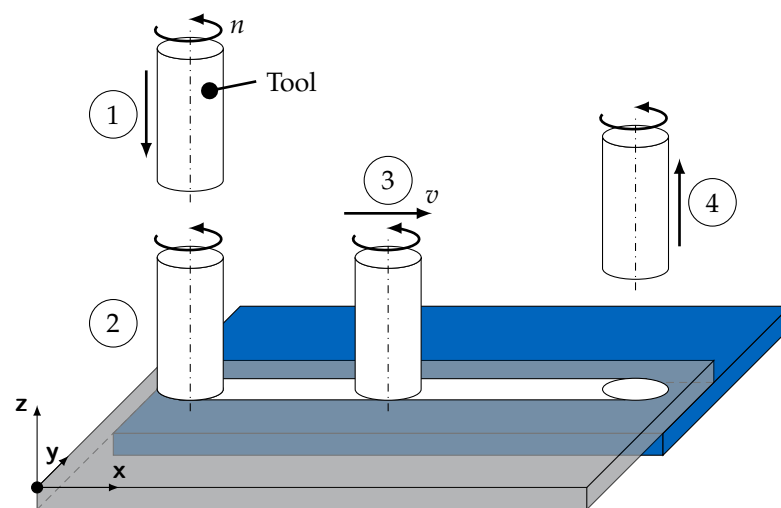


**Figure 1.** Process sequence of FPJ (blue, thermoplastic material; gray, aluminum), according to Meyer et al. [8].

The principle of direct joining with FSW-like processes is also known as Friction Lap Welding (FLW). However, FLW is usually not associated with surface pretreatment of the metallic joining partner [10]. Hence, in most studies, only polar plastics, such as polyamides, were employed. In addition to non-reinforced plastics, numerous fiber-reinforced (short and continuous fibers) plastics were joined via FLW and FPJ [11–13]. In most cases, various aluminum alloys were used as the metallic joining partner [11]. Notwithstanding, studies on the joining of copper specimens have also been reported [13].

## 2.2. Adhesive Bonding

The adhesive bonding of plastic and metal components is challenging due to many influences during the process, such as the air humidity, the curing time and the curing temperature, which all impact the resulting bond properties [14]. Nonetheless, adhesive bonding has become a standard procedure in the aircraft manufacturing industry to form joints in the body and the wing structures [2].

According to Arenas et al. [15], two main adhesive systems are used in the aircraft design for plastic-to-metal bonding: epoxy-based adhesives for high-strength static loads and polyurethane-based adhesives for dynamically stressed joints. These adhesive systems are characterized by their inherent properties, such as the rigidity (epoxy-based) or the flexibility (polyurethane-based). Regardless of the adhesive system used, surface pretreatment of the joining partners is a decisive factor that significantly influences the strength [16].

Furthermore, adhesive bonding is a standardized manufacturing process with a high technology readiness level (TRL) [2]. However, this process requires a high level of process control to minimize the environmental impact on the adhesive joint and quality control to ensure the bond strength.

## 2.3. Technology Readiness Level and Technology Potential

The technology readiness level method is a procedure to assess a technology's maturity and promote its further development [17]. This assessment provides the basis for an effective technology and innovation management for the industrial sector [18]. According to Mankins [17], the classification mainly used in aviation is divided into nine individual levels. The first two stages comprise the assessment of theoretical knowledge about a technology. TRL 3–5 consider the technical implementation from the proof of concept to the implementation in an industrial production environment. TRL 6 and 7 refer to the production of a prototype. TRL 8 and 9 apply to the implementation in an actual flight system. With the help of this very detailed classification, a categorization of novel manufacturing methods according to their operational readiness is possible. It should be noted that the transitions between the individual stages can be fuzzy.

Brousseau et al. [19] reduced this nine-step classification to a seven-step technology maturity assessment (TMA) model:

**Level 1** Basic technology research

**Level 2** Feasibility study

**Level 3** Technology development

**Level 4** Technology demonstration

**Level 5** System development/integration

**Level 6** Integration in a production environment and validation

**Level 7** Mass production/serial production

A technology profile developed using this method is valid for an individual company and provides a far-reaching overview of the entire technology itself [19].

Reinhart and Schindler [20] used the TRL approach of Mankins [17], the TMA model of Brousseau et al. [19] and the technological life cycle concept of Ford et al. [21] to develop a technology profile. This profile combines these methods and accounts for uncertainties of the given information. It was possible to quantify the linguistic criteria by using fuzzy logic, resulting in a seven-step technology profile to describe the overall technological maturity.

Based on these findings, Hofer et al. [22] examined the potential of novel production processes, such as the production of lithium-ion batteries and their impact on company policy. The approach was extended to include the technical aspects and the economic and strategic perspectives. According to Hofer et al. [22], these three elements form the technology potential, which can be used to evaluate a novel technology and estimate the possible benefits.

### 3. Experimental Material and Set-Up

#### 3.1. Experimental Material

To cover a broad spectrum of possible material combinations (MC), the experiments, which led to the findings of this paper, were conducted using three different types of plastic material in combination with two types of aluminum alloys (see Table 1). For a better overview, the material combinations analyzed in this paper are indicated by Roman numerals I–III in Table 1.

**Table 1.** Overview of the material combinations and the abbreviations used in this paper.

Material Combination		Abbreviation
EN AW-6082-T6	PE-HD	I
EN AW-6082-T6	PA6-GF30	II
EN AW-2024-T3	PPS-CF	III

Three semi-crystalline thermoplastics were chosen. The non-reinforced polyethylene (PE-HD) is a typical example of mass plastics. In contrast, the short fiber-reinforced polyamide (PA6-GF30) is an engineering plastic. As a variant of high-performance plastics, the endless fiber-reinforced polyphenylene sulfide (PPS-CF), often used in aircraft design [23], was chosen. This selection covers a wide range of mechanical and thermal properties, which are listed in Appendix A (see Table A2). All samples were purchased as sheet material from the corresponding suppliers.

The high-density polyethylene (PE-HD) distributed by S-Polytec GmbH, Germany, Goch has a low density, high crystallinity, non-polar character and excellent chemical resistance. Besides that, this group of plastics absorbs a minimal amount of water [24]. For these reasons, these polymers are used in many applications, e.g., as micro-granules for additive manufacturing [25] and implants [26]. The thickness of the material was 5 mm.

The second plastic used was a polyamide 6 with 30 % glass fiber content (PA6-GF30), supplied by Ensinger GmbH, Germany, Nufringen, under the trade name TECAMID 6 GF30 black [27]. This group of plastics is known for its polar nature and high strength. Therefore, it is the subject of various research projects in joining technology [28]. The thickness of the material was 5 mm.

The endless carbon-fiber-reinforced (43 wt%) polyphenylene sulfide (PPS-CF) used is a semi-crystalline high-performance thermoplastic sold by TenCate Advanced Composites B.V., The Netherlands, Nijverdal, under the brand name CFK Cetex TC1100. The fibers in the laminate are arranged in a 5H-satin configuration and laid in seven layers [(0/90), ( $\pm 45$ )<sub>3</sub> (0/90)]. High heat resistance, high chemical resistance and high stiffness characterize this fiber-matrix composite. Hence, it has been widely used in aerospace applications [23,29] and research [30]. The material thickness is derived from the above-mentioned layer structure and was 2.17 mm [31].

The main aluminum alloy under study was an EN AW-6082-T6 [32], as used in several publications on friction press joining [8,9,33]. The thickness was 3 mm.

The second aluminum alloy, a hardenable, high-strength EN AW-2024-T3 [34], is frequently employed in aircraft manufacturing [35]. Due to its poor welding properties and low corrosion resistance, this alloy is usually adhesively bonded. The sheet thickness was 2 mm.

#### 3.2. Surface Pretreatment

To compare the two technologies (FPJ and adhesive bonding), three different plastic–metal combinations were joined. For both processes, the surface pretreatment is a significant influencing factor affecting the resulting bond strength [8,16]. According to Wirth et al. [9], laser-based surface pretreatment is advantageous compared to other methods, because of the absence of chemicals as well as the fast and contact-free processing. For these reasons, the surfaces of the metallic joining partners were modified by laser radiation. Based on Meyer

et al. [8], a quasi-chaotic nanostructure was produced (see Figure 2) on both aluminum alloys. This structure exhibits a highly porous oxide layer as well as directional independence. It was generated using a pulsed laser system (Rofin-Sinar PowerlineF20) with a wavelength of 1064 nm (see Table 2). Compared with Lambiase [36], we used a different laser system for surface pretreatment, which differs mainly in the pulse duration. In [36], small cutting edges were created, while the surface modification used here utilizes the oxide layer that is formed. A major advantage of this method is the fact that a considerably faster process is obtained with two exposures, while [36] required 20 exposures.

**Table 2.** Laser structuring parameters for the generation of a quasi-chaotic nanostructure.

Parameter	Unit	Value
Power $P$	W	20
Frequency $f$	kHz	20
Exposures $n$	–	2
Pulse spacing $p_s$	$\mu\text{m}$	25
Focus diameter $d_{foc}$	$\mu\text{m}$	50
Pulse energy $E_P$	mJ	1

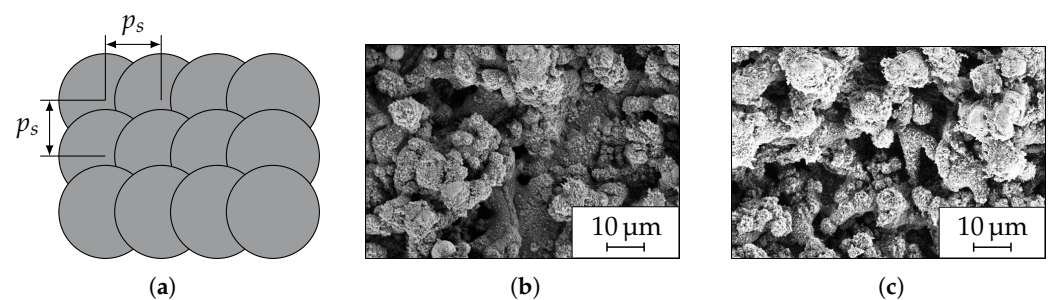


**Figure 2.** Illustration of the pulse pattern for a chaotic nanostructure (a) and scanning electron microscope (SEM) images (acceleration voltage of 1 kV) of the generated structures on EN AW-2024-T3 (b) and EN AW-6082-T6 (c).

The surface of the plastics was cleaned with ethanol to remove any grease and other contamination. The surface was not pre-treated mechanically or physically.

### 3.3. Selection of the Adhesives and Bonding

For the adhesive joining of the three material combinations, different adhesive systems were used to obtain the maximum strength (see Table 3). The selection of the adhesives is based on a literature review and consultation with the respective manufacturers. The investigated adhesives are used either in this way or in a similar configuration, in industrial applications.

**Table 3.** Overview of the material combinations, the used adhesive (A) and their abbreviation used in this paper.

MC	Adhesive	Category	Abbreviation
I	Scotch Weld DP 8005	Acrylic-based	I-A
II	DELO 02 rapid	Epoxy resin	II-Aa
	DELO AD 948	Polyurethane	II-Ab
III	Loctite EA 9466	Epoxy resin	III-A

A two-component acrylic-based adhesive system [37] was utilized for the material combination of PE-HD and aluminum. Oguma and Naito [38] used an acrylic-based Scotch-Weld DP8005 supplied by 3M to join glass fiber-reinforced polypropylene samples

to each other. As polyethylene is very similar to polypropylene (in terms of its chemical structure), this adhesive system was selected.

To bond the polar polymer PA6-GF30, two different adhesive systems were used according to Arenas et al. [15]: a two-component epoxy-based system (DELO 02 rapid) [39] and a two-component polyurethane-based adhesive (DELO AD 948) [40].

For the high-strength bonds of PPS-CF and EN AW-2024-T3, the two-component epoxy-based adhesive Loctite EA 9466 [41] from the Henkel AG was chosen, following Spaggiari and Dragoni [42] and Soykok [43].

To ensure reproducibility, all adhesive bonds were executed twice. For a better overview, the adhesive systems are designated in the following with the proposed material combination (I–III), a hyphen and an *A* for adhesive. For Combination II, there is both an epoxy-based (Aa) and a polyurethane-based (Ab) adhesive system (see Table 3).

The layer thickness of the adhesives was set to approximately 250  $\mu\text{m}$ . For bonding with II-Aa only, a layer thickness of approximately 100  $\mu\text{m}$  was selected. The curing was performed at room temperature (approximately 23  $^{\circ}\text{C}$ ) for 120 h.

### 3.4. FPJ System, Clamping and Parameters

The FPJ experiments were conducted on a Heller MCH 250 CNC milling machine (Workspace of 800 mm  $\times$  800 mm  $\times$  800 mm). The main spindle is positioned horizontally on this machine and can be moved in the *x*- and the *y*-direction. The tilt angle  $\alpha$  between the tool and the workpiece can be adjusted by rotating the clamping base around the *b*-axis. This clamping base can be moved in the *z*-direction and provides a maximum force of 30 kN with a positioning accuracy of 0.001 mm. The FPJ specimens were mounted on the clamping base using a customized clamping system made of C45 steel with a base thickness of 35 mm (see Figure 3). The tool used was made of XCrMoV5, had a diameter of 25 mm and a flat front face. The process was conducted by using the force control presented in [11].

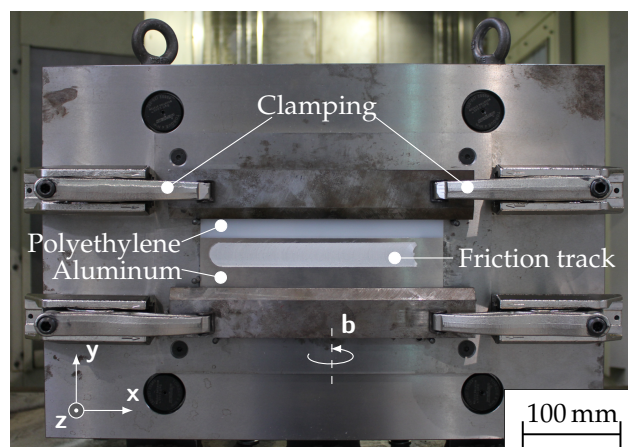


**Figure 3.** Customized clamping system for joining aluminum and thermoplastic material (in this case polyethylene) by friction press joining [11].

The parameters used for the FPJ experiments were based on previous investigations [8,9] and are listed in Table 4. For a better overview, roman numerals combined with a PS (I-PS–III-PS) indicate the parameter sets (PS) for joining the different material combinations (see Table 4). Each parameter set was conducted twice.

**Table 4.** Parameter sets for the FPJ experiments for each material combination and their used abbreviation (abbr.); all experiments were conducted with a tilt angle  $\alpha$  of 2°.

MC	Rot. Speed $n$ in $\text{min}^{-1}$	Feed Rate $v$ in $\text{mm min}^{-1}$	Ax. Force $F_a$ in N	Abbr.
I	400	150	2000	I-PSa
	600	600	2000	I-PSb
	800	450	2000	I-PSc
	800	600	2000	I-PSd
	1000	750	2000	I-PSe
II	600	400	2000	II-PSa
	600	560	2000	II-PSb
	800	240	2000	II-PSc
	800	600	2000	II-PSd
III	1500	450	2500	III-PSa
	2000	300	2500	III-PSb
	2500	300	2500	III-PSc

### 3.5. Test Geometry and Tensile Shear Tests

For both the bonding process and the FPJ process, the same sample dimensions were used for each material combination (I–III). In each case, two plates measuring 100 mm  $\times$  250 mm were joined with an overlap of 35 mm. For the FPJ-experiments, the seam length was 200 mm, while the adhesive samples' bonding was over the entire contact surface. Five 25 mm-wide tensile shear specimens were prepared out of the middle of the joined plates, resulting in a total overlap of 875 mm<sup>2</sup> for a single test sample. These specimens were used for the tensile lap shear test on a material testing machine Z050 (Zwick/Roell, Germany, Ulm). The initial length  $l_0$  for this test was 115 mm. The traverse speed was set to 50 mm min<sup>-1</sup> for the combination of PE-HD and aluminum and 5 mm min<sup>-1</sup> for the other material combinations.

## 4. Results and Discussion of the Experiments

### 4.1. Comparison of the Bond Strengths

The strength of the composites produced by FPJ were similar or higher than the strength of the reference samples joined by adhesives (see Figure 4). For a better overview, only the results of the best FPJ parameter set for the corresponding material combination are shown in Figure 4. The results of all individual experiments are supplied in the Appendix A in Tables A3 and A4.

For the material combination PE-HD and EN AW-6082-T6 (I), the composites produced with FPJ showed the same tensile shear strength as the adhesive composites. Here, the total adhesive forces exceeded the internal strength of the plastic joining partner. Therefore, the maximum strength did not lead to the joint's breakage but led to the elongation of the plastic and its material hardening due to the alignment of the macromolecules (strain hardening) (see Figure 5). The shown tensile shear strengths of approximately 2700 N thus refer to the stress area (cross-section of plastic joining partner) of 125 mm<sup>2</sup>. The measured stress value of 21.6 MPa correlates well with the value of 23 MPa given in the datasheet (see Table A2). To be able to investigate the joint strength more closely, the overlap length should be reduced in further investigations in order to obtain a fracture in the joining zone.

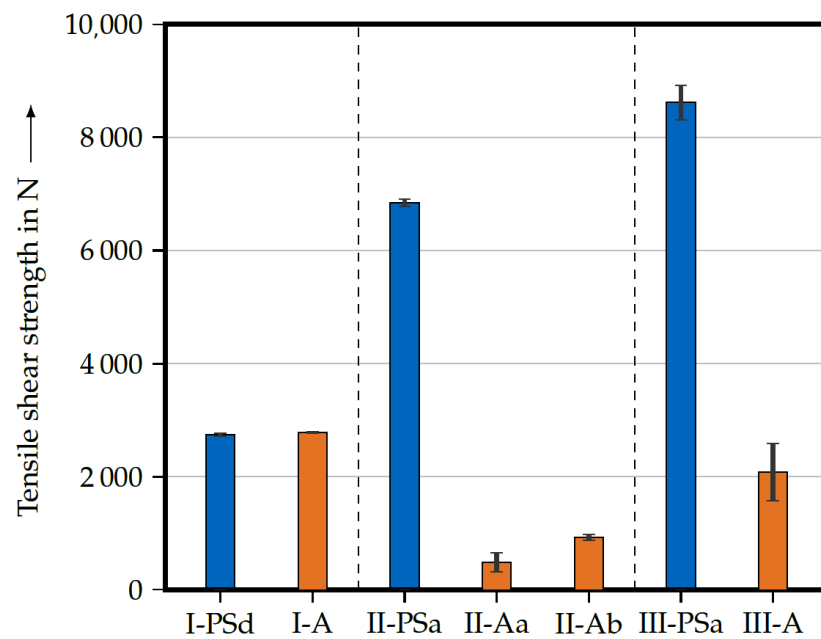


**Figure 4.** Tensile shear strengths of selected joints (blue, FPJ; orange, adhesive bond) including the standard deviation of five tensile shear specimens.



**Figure 5.** Typical FPJ tensile shear test specimen made of PE-HD and EN AW-6082-T6 (I-PSd) after a successful lap shear test with distinct strain hardened area.

The FPJ bonds for the material combination of PA6-GF30 and EN AW-6082-T6 (II) showed a significantly higher bond strength than the reference samples (adhesive bonding) (see Figure 4). In all cases, the plastic joining partner broke at the edge of the metallic joining partner (see Figure 6). Concerning the stress cross-section (cross-section of the plastic joining partner), the strength is 54.4 MPa, approximately 55 % of the value specified on the datasheet. This reduced maximum tensile strength of the plastic joining partner can be explained by a certain notch effect at the transition between the plastic and the metal (see Figure 6a). As the end of the metal sheet is pressed into the plastic, the real cross-sectional area is reduced and a sharp-edged transition is created. Another possible explanation could be the thermal degradation of the plastic, which would also weaken the bond strength. For the adhesive bond, a purely adhesive break between the plastic and the adhesive film occurred. This fracture pattern showed that the bond between the pretreated metal and the adhesive is high. In contrast, the bond between the adhesive and the plastic is weak. Since the plastic surface was not pretreated except for a surface cleaning (ethanol), no mechanical adhesion (form closure) could develop. Based on the results of Don R. [44], it is assumed that due to the molecular structure of the polymer chains of the plastic, neither the epoxy-based nor the polyurethane-based adhesive can form chemical bonds (missing the reactive end groups) with the plastic. For this reason, the authors see an advantage in the FPJ process for the material combination of polyamide and aluminum.

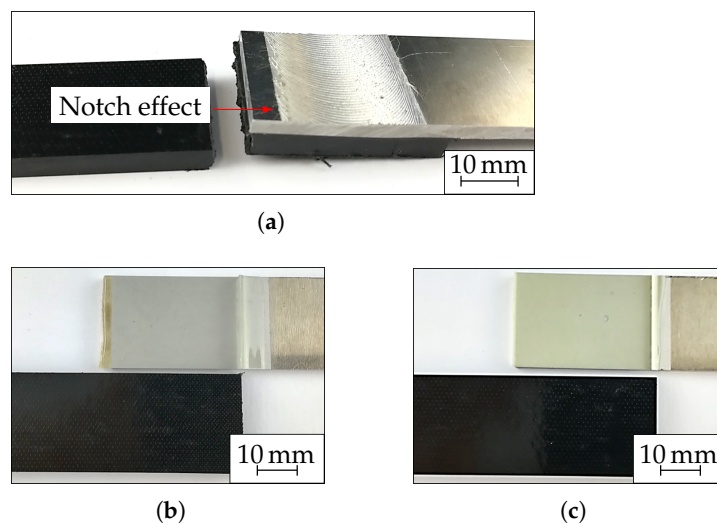


**Figure 6.** Comparison of the surfaces at fracture of PA6-GF30 and EN AW-6082-T6 joined with: FPJ (II-PSa) (a); epoxy-based adhesive (b); and polyurethane-based adhesive (c).

The strengths of the combination PPS-CF and EN AW-2024-T3 (III) also demonstrate the benefit of FPJ. The fracture pattern of the FPJ bonds showed that the bond between the plastic and the metal was high (plastic remains on the metal surface) and the bond between the plastic and the fibers was the weak point (see Figure 7a). Moreover, not the entire joining surface was heated and thus bonded (see Figure 7a). As a result, the fracture pattern can be separated into an area where the PPS was not melted, an area where the bond failed cohesively, and an area where the bond failed adhesively. Since joining the entire surface was not possible, the actual stress in the bond was significantly higher. Therefore, the potential of the FPJ process was not fully exploited. To counteract this effect, the heat input into the bond should be improved further to plasticize the entire joining surface and increase its strength. In contrast, joints produced by adhesive bonding show a distinctive adhesive fracture between the epoxy-based adhesive and the plastic. Similar to material combination II, the bond between the plastic and the adhesive was a weak point in the composite. Therefore, FPJ is considered to be an advantageous process to join the material combination III.

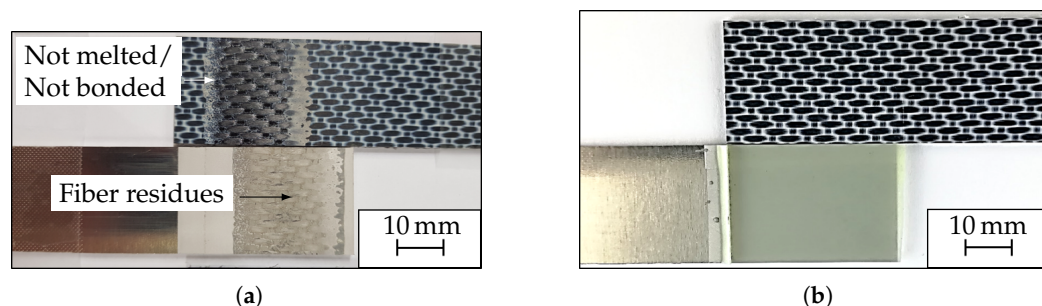


**Figure 7.** Comparison of the 25 mm wide samples after the tensile test: (a) joined with parameter set III-PSa; and (b) joined with an epoxy-based adhesive.

In summary, the FPJ joints display an equivalent or even higher mechanical strength compared to adhesive bonding. To characterize the actual bond, the overlap length should be reduced in future studies, at least for the material combination of PE-HD or PA6-GF30 with EN AW-6082-T6, to achieve a fracture in the joining surface in the tensile tests. Only a qualitative result could be derived from the tests presented within this study.

#### 4.2. Comparison of the Cross-Sections

After analyzing the tensile shear strengths and fracture surfaces, the cross-sections of the individual samples were compared (see Figure 8).

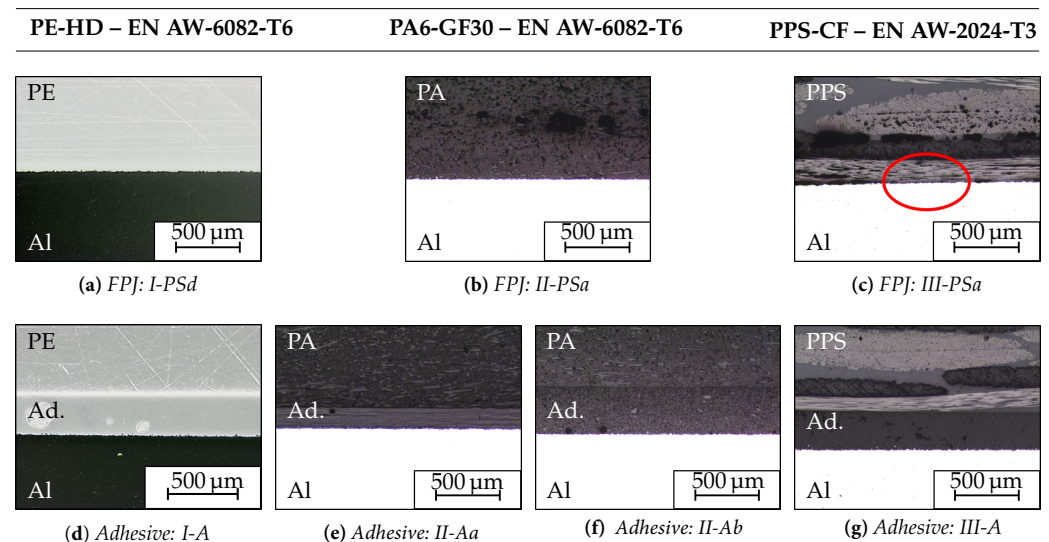


**Figure 8.** Cross-sections of the joining zones for the three considered material combinations and the two joining processes; the captions of the individual images refer to the process parameters used or the applied adhesive. To achieve a better visibility of the layered structure, the contrast of the microscopic images was increased, which causes a side effect: the aluminum appears black (a,d) or white. The adhesive layer is indicated as *Ad.*

For the FPJ bonds shows, it can be seen, that the plastic interacts directly with the pretreated surface of the aluminum. For the connection with PPS-CF (see Figure 8c), it can be seen that, due to the low matrix content, the fibers (light gray) partially touch the metal (see red circle). This effect can also be observed on the fracture surface of the tensile tests (see Figure 7a), where fiber remains on the surface of the metal. Generally, by melting the plastic, it can interact with the pretreated aluminum surface and form high-strength bonds.

For all adhesive joints (see Figure 8d–g), a layered structure consisting of aluminum (Al.), adhesive (Ad.) and plastic (PE, PA or PPS) was identified. The adhesive penetrates the pretreated aluminum surface and thus forms a mechanical interlock. A sharp separation between the plastics PA6-GF30 and PPS-CF and the corresponding adhesives is visible. This separation indicates that the plastic was not chemically affected, and only weak physical bonds exist. However, for the plastic PE-HD (see Figure 8d), a small intermediate layer is visible. Here, it appears that a reaction has taken place between the plastic and the adhesive (acrylic-based). The analysis of the fracture patterns confirms these observations. The adhesive bonds between thermoplastics and metals only occur when the plastic is chemically treated.

#### 4.3. Comparison of the Surface Quality

During FPJ, the tool is guided along the surface of the metallic joining partner (see Figure 1). This processing leads to a so-called friction track on the surface (similar to an FSW seam) (see Figure 9). The term *seam* is avoided here since the actual seam is located at the interface between the metal sheet and the plastic component. This distinctive feature determines the visual appearance of the bond.

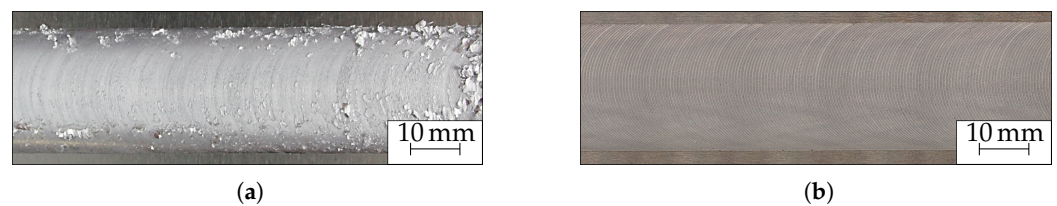


**Figure 9.** Comparison of the friction tracks (25 mm in width) between the aluminum alloy EN AW-2024-T3 (a) processed with parameter set III-PSb and EN AW-6082-T6 (b) produced with parameter set II-PSa.

In general, the alloy EN AW 2024-T3 showed superficial flaking with a small aluminum layer peeled off (see Figure 9a). As a result, the characteristic arc texture formation is not distinct. This behavior is not yet understood. To exclude an influence of the process parameters, additional tests with similar feed rates and rotational speeds were performed. A reduced superficial flaking formation was observed for the alloy EN AW 2024-T3. For this reason, it can be assumed that the material has a more significant influence on the quality of the friction surface, although the process parameters permit a certain adjustment of its quality. In contrast, no delamination could be detected for the alloy EN AW-6082-T6 (see Figure 9b). Other surface defects known from FSW [45], such as surface galling, were only observed sporadically. However, since the friction track is a characteristic optical feature, this aspect should be considered more closely for industrialization purposes.

## 5. Technical Maturity

### 5.1. Technology Readiness Level of FPJ

As outlined in the Introduction, the technological maturity is a crucial aspect for the industrialization of a technology. To be able to compare the technological and economic aspects, it is essential to evaluate the maturity of a new technology. Therefore, the TRL of FPJ is discussed hereafter.

To assess the technological maturity of FPJ, the state of the art was evaluated. Furthermore, 15 experts on FPJ, FLW and FSW discussed this topic in two meetings, according to the method of Reinhart and Schindler [20] (as the evaluation forms published in [20], which serve as a basis for the assessment, are too extensive to be included in this paper, please feel free to ask the author for the data). As described in Section 2.3, the maturity model comprises seven levels, representing different stages of a technology's evolution. The technology readiness, according to the maturity levels for the analyzed joining process (FPJ), is shown in Figure 10. The diagram is structured according to the phases (vertical) and the maturity levels (horizontal). The error bars show the uncertainty contained in the answers of the experts.

Levels 1 and 2 (basics) indicate an advanced state of progress. Thus, the theoretical background on FPJ is well known, and the correlation between the individual process parameters is generally understood. This status is also confirmed by the numerous publications regarding FPJ or FLW (see Section 2).

Levels 3 and 4 represent a high degree of progress. This advanced stage illustrates that the development and the validation of the technology are well advanced. Furthermore, prototype components have already been produced. Therefore, the development of the technology and the validation on a laboratory scale can be classified as sufficiently advanced. Up to now, only plane surfaces (sheets) have been joined. However, the geometry flexibility is considered to be similar to FSW, thus it can be assumed that curved surfaces can also be joined ([46] pp. 131–133).

The integration into an operating resource, assessed for Level 5, can also be classified as sufficient, partly because the FPJ process relies on similar resources to the FSW process. In the further qualification of the technology for series production in Level 6 (production structure) and optimization in the series production (Level 7), a clear decline in the degree of progress can be seen. The high standard deviation for Level 6 indicates high uncertainties

in identifying the characteristics in the production environment. The low progress value indicates that the technology is still hardly established in industrial production, but it is increasingly perceived as an alternative to other joining processes. It should be noted that up to now there are no publications concerning lifetime/fatigue tests of the FPJ/FLW bonds, nor studies dealing with the mechanical properties at increased or low temperatures ( $-60$  to  $60$  °C).

To calculate the overall maturity of the technology and to indicate uncertainties in the evaluation, a Monte Carlo simulation with 1000 runs was conducted. A more detailed description of the method used is given in Reinhart and Schindler [20]. With an average value of around  $61 \pm 6\%$ , an advanced development stage of the FPJ technology was identified. This result shows that this novel technology is already well advanced and on the verge of entering the industrial production environment.

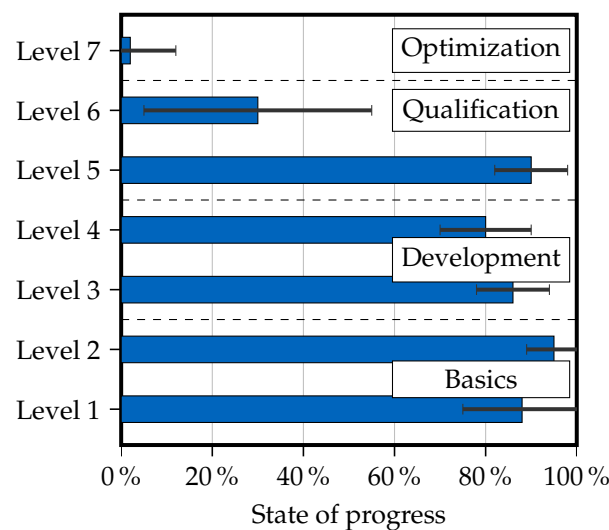


**Figure 10.** Level of maturity according to the individual development stages, based on the method of Reinhart and Schindler [20].

### 5.2. Technology Potential of FPJ

To evaluate the technology potential, the economic and company-strategic aspects should be considered in addition to the mentioned technical perspective. Consequently, only the economic points are discussed hereafter since the authors are unable to cover company-strategic approaches.

According to Hofer et al. [22], economic conditions include the cost-cutting potential, the revenue-increase potential and the economic potential. These three topics with respect to the technology covered by this paper are summarized shortly in the following. The possibility of direct joining of plastic components and metals eliminates the need for adhesives. The time saved due to the elimination of curing time must be weighed against the joining time required for the FPJ. This time depends on the material as well as on the geometry. In general, it can be assumed that a reduction of the production time is possible, especially compared to epoxy-based adhesives (curing time of 24 h at room temperature [39]). Due to the trend in aircraft design to replace thermosetting materials with thermoplastic materials [29], there is also an increasing number of new scenarios for applying friction press joining. The elimination of the adhesive, and thus the reduction of the total mass, result in a significant cost advantage over the aircraft's lifetime, which can compensate for the higher cost of the system technology (CNC machine center, meteorology and software) used for FPJ. The reduction of the total mass leads to a reduction in the fuel consumption. In particular, the fuel economy is essential for new aircraft's sales prices, which is why an increase in the profit can be expected when using the FPJ technology.

These considerations indicate the high economic potential of FPJ for specific joining processes. Together with the already existing high technological maturity, only minor risks arise for the application of this technology in the industrial context.

## 6. Classification of the FPJ Process

Finally, after discussing the technological and economical aspects, this paragraph deals with the classification and categorization of the FPJ process into the DIN 8580 [47] standard. In the following section, a proposal is discussed to classify the process based on the current knowledge in the literature (see Figure 11).

The objective of the classification is to promote the advancement of the joining process based on the current data available rather than constraining it within a specific manufacturing processing. It is possible that the category of the process needs to be redefined or new sub-categories need to be proposed to more accurately describe the process.

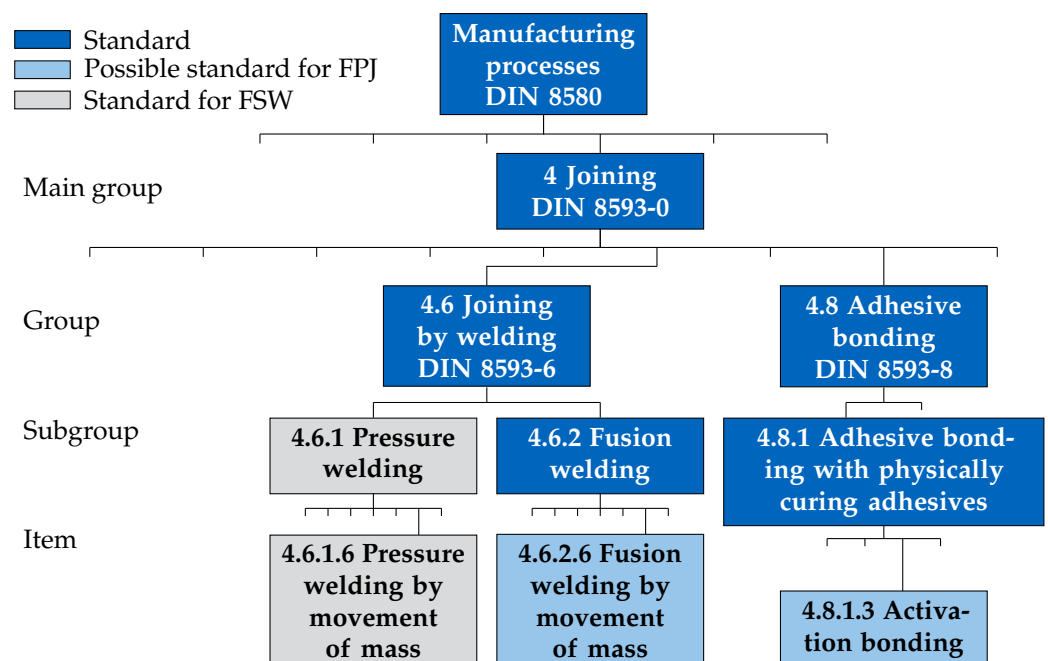


**Figure 11.** A recommendation for the classification of the friction press joining process according to the DIN 8580 [47] standard for manufacturing processes.

Friction press joining is a manufacturing process for joining thermoplastic materials and metal sheets. Thus, it belongs to the fourth main group *Joining*, defined in DIN 8593-0 [47,48]. The related process *friction stir welding* (FSW), from which FPJ was derived, is standardized in DIN EN ISO 25239-1 [49] and assigned to *Pressure welding* (1st subgroup) under DIN 8593-6 [50] (*Joining by welding*). Pressure welding is subdivided further according to DIN 1910-100 [51], where the FSW process is classified in item 4.6.1.6 *Pressure welding by movement of mass* [50]. However, since one joining partner (the thermoplastic material) has to be melted during friction press joining, it is not classifiable as a pressure welding process, according to DIN 8593-6 [50].

In the second subgroup, 4.6.2 *Fusion welding* (DIN 8593-6 [50]), item 4.6.2.6 *Fusion welding by movement of mass* would be a possible alternative. Thus far, no processes are listed under this item. An essential criterion for the classification in this item is the type of the bond. According to Wirth et al. [9], FPJ is based on micro-form-closure, and according to Meyer et al. [8] on micro-form-closure and Van der Waals forces. As these two phenomena are based on cohesive forces, a classification in this category is conceivable. In addition, Liu et al. [10,52] showed that Al-O-C bonds were formed at the aluminum/polyamide interface. Here, the carbonyl group at the PA66 surface was essential for the formation of this a bond mechanism. This type of formation proved to be a key factor to achieve a

high joint strength. It provided also an explanation why aluminum alloys can be directly welded to PA66 plates with a high joint strength.

Based on the bonding mechanisms, a second possibility is a classification according to DIN 8593-8 (Adhesive bonding) [53]. For FPJ, the plastic serves as a joining partner, as well as an adhesive. During the process, the heat input is conducted externally through friction into the metallic joining partner and through conduction into the joining zone, causing the adhesive (plastic) to be melted. Therefore, this process can be seen as a hot-melt process, which belongs to 4.8.1.3 *Activation bonding*.

In summary, an indexing to *Fusion welding by movement of mass* (item 4.6.2.6) and an assignment to *Activation bonding* (item 4.8.1.3) is conceivable. Since FPJ can be seen as a hot-melt process, the authors recommend classifying FPJ as *Activation bonding*. For this reason, we use the term *joining* or *bonding*, instead of welding.

## 7. Summary, Conclusions and Outlook

In the context of this publication, a benchmark study was conducted on friction press joining and adhesive bonding of plastic–metal composites. Different adhesive systems were selected, and their resulting tensile strengths were compared to the strengths of the friction-press-joined reference samples. It was found that the direct bonds showed higher or at least equivalent tensile strengths compared to the samples joined with adhesives.

In addition to this technical aspect, the technological maturity and potential were evaluated. The analyses revealed that the FPJ technology is well advanced and near of its application in industry. Altogether, the following main conclusions can be formulated:

- C1 The achieved maximum tensile shear strengths for the studied material combinations joined by FPJ are higher than those of the comparative samples joined by adhesive bonding.
- C2 The overall technological maturity of friction press joining was rated as  $61 \pm 6\%$ . Thus, the technology is ready to be embedded in an industrial production environment.
- C3 The technological potential to replace adhesive bonding in aircraft design can be classified as high.
- C4 A classification of the process (FPJ) according to DIN 8593-0 into *Activation bonding* (item 4.8.1.3) is conceivable.

This benchmark study forms the basis for a validation in an actual production environment of mass products. Besides that, a detailed economic evaluation of the processes should confirm the discussed cost-saving potential. An additional key aspect for future studies is to investigate the long-term mechanical properties under the influence of temperature in order to qualify the FPJ technology for aircraft.

**Author Contributions:** Conceptualization, S.P.M.; methodology, S.P.M.; validation, S.P.M. and M.T.H.; formal analysis, S.P.M. and M.T.H.; investigation, S.P.M. and M.T.H.; resources, S.P.M. and J.B.H.; data curation, S.P.M. and M.T.H.; writing—original draft preparation, S.P.M. and J.B.H.; writing—review and editing, J.B.H. and M.F.Z.; visualization, S.P.M.; supervision, S.P.M.; project administration, S.P.M.; and funding acquisition, S.P.M., J.B.H. and M.F.Z. All authors have read and agreed to the published version of the manuscript.

**Funding:** This work was funded by the Deutsche Forschungsgemeinschaft (DFG, German Research Foundation) (418104776).



**Institutional Review Board Statement:** Not applicable.

**Informed Consent Statement:** Not applicable.

**Conflicts of Interest:** The authors declare no conflict of interest.

## Appendix A

The Appendix lists all tensile test experiments (see Tables A3 and A4) and the material properties of the used components (see Tables A1 and A2).

**Table A1.** Selected thermal and mechanical properties of the aluminum EN AW-6082-T6 and EN AW-2024-T3 [32,34,54].

Property	Unit	EN AW	
		6082	2024
Condition	–	T6	T3
Tensile strength $R_m$	$\text{N mm}^{-2}$	300–350	435
Yield strength $R_{p0.2}$	$\text{N mm}^{-2}$	240–320	290
Elongation at fracture $A_{50mm}$	%	8–14	14
Young's modulus $E$	MPa	70,000	70,000
Density $\rho$	$\text{g cm}^{-3}$	2.70	2.77
Melting range $T_m$	$^{\circ}\text{C}$	585–650	505–640
Thermal conductivity $\lambda$	$\text{W m}^{-1} \text{K}^{-1}$	150–185	130–150
Coefficient of linear thermal expansion $\alpha$	$10^{-6} \text{K}^{-1}$	23.4	22.9

**Table A2.** Selected mechanical and thermal properties of the plastic components used [24,27,31].

Property	Unit	PE-HD	PA6-GF30	PPS-CF
Tensile strength $R_m$	$\text{N mm}^{-2}$	23	98	752–785
Yield strength $R_{p0.2}$	$\text{N mm}^{-2}$	–	98	608
Elongation at fracture $A$	%	–	5	–
Young's modulus $E$	MPa	1100	5700	56,000–58,000
Density $\rho$	$\text{g cm}^{-3}$	0.96	1.36	1.55
Crystallization temperature (range) $T_c$	$^{\circ}\text{C}$	126–130	218	280
Thermal conductivity $\lambda$	$\text{W m}^{-1} \text{K}^{-1}$	0.38	0.41	–
Coefficient of linear thermal expansion $\alpha$	$10^{-4} \text{K}^{-1}$	1.8	0.6	–

**Table A3.** Lap shear test results for all FPJ joined specimens.

MC	Abbr.	Tensile Strength in N	Standard Deviation $\sigma$ in N
I	I-PSa	2576.3	173.85
	I-PSb	2710.0	53.88
	I-PSc	2716.8	17.77
	I-PSd	2742.2	24.67
	I-PSe	2745.8	12.92
II	II-PSa	6844.4	67.51
	II-PSb	6606.8	202.57
	II-PSc	6199.4	194.48
	II-PSd	6478.6	148.96
III	III-PSa	8613.6	308.01
	III-PSb	7289.2	530.86
	III-PSc	7046.6	564.89

**Table A4.** Lap shear test results for all adhesively bonded specimens.

MC	Abbr.	Tensile Strength in N	Standard Deviation $\sigma$ in N
I	I-A	2785.0	12.76
II	II-Aa	489.0	170.01
	II-Ab	924.8	51.39
III	III-A	2082	501.20

## References

1. Marsh, G. Airbus A350 XWB update. *Reinf. Plast.* **2010**, *54*, 20–24. [\[CrossRef\]](#)
2. Higgins, A. Adhesive bonding of aircraft structures. *Int. J. Adhes. Adhes.* **2000**, *20*, 367–376. [\[CrossRef\]](#)
3. Hertle, S.; Kleffel, T.; Wörz, A.; Drummer, D. Production of polymer-metal hybrids using extrusion-based additive manufacturing and electrochemically treated aluminum. *Addit. Manuf.* **2020**, *33*, 101135. [\[CrossRef\]](#)
4. Lucchetta, G.; Marinello, F.; Bariani, P.F. Aluminum sheet surface roughness correlation with adhesion in polymer metal hybrid overmolding. *CIRP Ann.* **2011**, *60*, 559–562. [\[CrossRef\]](#)
5. Arai, S.; Sugawara, R.; Shimizu, M.; Inoue, J.; Horita, M.; Nagaoka, T.; Itabashi, M. Excellent bonding strength between steel and thermoplastic resin using roughened electrodeposited Ni/CNT composite layer without adhesives. *Mater. Lett.* **2020**, *263*, 127241. [\[CrossRef\]](#)
6. Balle, F.; Wagner, G.; Eifler, D. Ultrasonic Metal Welding of Aluminium Sheets to Carbon Fibre Reinforced Thermoplastic Composites. *Adv. Eng. Mater.* **2009**, *11*, 35–39. [\[CrossRef\]](#)
7. Emrich, N.; Meyer, S.P.; Daub, R. Ageing behavior of thermally joined hybrids of laser pre-treated metal and thermoplastic polymers. In Proceedings of the 35th International Conference of the Polymer Processing Society (Pps-35), Çeşme-Izmir, Turkey, 26–30 May 2019; AIP Publishing: New York, NY, USA, 2020; p. 020001. [\[CrossRef\]](#)
8. Meyer, S.P.; Wunderling, C.; Zaeh, M.F. Influence of the laser-based surface modification on the bond strength for friction press joining of aluminum and polyethylene. *Prod. Eng.* **2019**, *13*, 721–730. [\[CrossRef\]](#)
9. Wirth, F.X.; Zaeh, M.F.; Krutzlinger, M.; Silvanus, J. Analysis of the Bonding Behavior and Joining Mechanism during Friction Press Joining of Aluminum Alloys with Thermoplastics. *Procedia CIRP* **2014**, *18*, 215–220. [\[CrossRef\]](#)
10. Liu, F.C.; Liao, J.; Nakata, K. Joining of metal to plastic using friction lap welding. *Mater. Des.* **2014**, *54*, 236–244. [\[CrossRef\]](#)
11. Meyer, S.P.; Bernauer, C.J.; Grabmann, S.; Zaeh, M.F. Design, evaluation, and implementation of a model-predictive control approach for a force control in friction stir welding processes. *Prod. Eng.* **2020**, *54*, 20. [\[CrossRef\]](#)
12. Nagatsuka, K.; Yoshida, S.; Tsuchiya, A.; Nakata, K. Direct joining of carbon-fiber-reinforced plastic to an aluminum alloy using friction lap joining. *Compos. Part B Eng.* **2015**, *73*, 82–88. [\[CrossRef\]](#)
13. Wu, L.H.; Nagatsuka, K.; Nakata, K. Direct joining of oxygen-free copper and carbon-fiber-reinforced plastic by friction lap joining. *J. Mater. Sci. Technol.* **2018**, *34*, 192–197. [\[CrossRef\]](#)
14. Custódio, J.; Broughton, J.; Cruz, H. A review of factors influencing the durability of structural bonded timber joints. *Int. J. Adhes. Adhes.* **2009**, *29*, 173–185. [\[CrossRef\]](#)
15. Arenas, J.M.; Alía, C.; Narbón, J.J.; Ocaña, R.; González, C. Considerations for the industrial application of structural adhesive joints in the aluminium-composite material bonding. *Compos. Part B Eng.* **2013**, *44*, 417–423. [\[CrossRef\]](#)
16. Zimmermann, S.; Specht, U.; Spieß, L.; Romanus, H.; Krischok, S.; Himmerlich, M.; Ihde, J. Improved adhesion at titanium surfaces via laser-induced surface oxidation and roughening. *Mater. Sci. Eng. A* **2012**, *558*, 755–760. [\[CrossRef\]](#)
17. Mankins, J.C. *Technology Readiness Levels; A White Paper*; Office of Space Access and Technology, NASA: Greenbelt, MD, USA, 1995.
18. Cetindamar, D.; Phaal, R.; Probert, D. Understanding technology management as a dynamic capability: A framework for technology management activities. *Technovation* **2009**, *29*, 237–246. [\[CrossRef\]](#)
19. Brousseau, E.; Barton, R.; Dimov, S.; Bigot, S. A Methodology for Evaluating the Technological Maturity of Micro and Nano Fabrication Processes. In *Precision Assembly Technologies and Systems*; Ratchev, S., Ed.; Springer: Berlin/Heidelberg, Germany, 2010; pp. 329–336.
20. Reinhart, G.; Schindler, S. A Strategic Evaluation Approach for Defining the Maturity of Manufacturing Technologies. *Int. J. Ind. Manuf. Eng.* **2010**, *4*, 1291–1296.
21. Ford, D.; Ryan, C. Taking technology to market. *Harv. Bus. Rev.* **1981**, *59*, 117–126.
22. Hofer, A.; Schnell, J.; Beck, B.; Reinhart, G. Potential-based Technology Planning for Production Companies. *Procedia CIRP* **2019**, *81*, 1400–1405. [\[CrossRef\]](#)
23. Amancio-Filho, S.T.; dos Santos, J.F. Joining of polymers and polymer-metal hybrid structures: Recent developments and trends. *Polym. Eng. Sci.* **2009**, *49*, 1461–1476. [\[CrossRef\]](#)
24. S-POLYTEC GmbH. *Technical Data Sheet: PE-HD*; S-POLYTEC GmbH: Goch, Germany, September 7, 2019.
25. Schäfer, C.; Meyer, S.P.; Osswald, T.A. A novel extrusion process for the production of polymer micropellets. *Polym. Eng. Sci.* **2018**, *44*, 1391. [\[CrossRef\]](#)

26. Kurth, M.; Eyerer, P.; Ascherl, R.; Dittel, K.; Holz, U. An evaluation of retrieved UHMWPE hip joint cups. *J. Biomater. Appl.* **1988**, *3*, 33–51. [[CrossRef](#)] [[PubMed](#)]
27. Ensinger Ltd. *TECAMID 6 GF30 Black—Stock Shapes*; Ensinger Ltd.: Nufringen, Germany, 2019.
28. Wolf, M.; Kleffel, T.; Leisen, C.; Drummer, D. Joining of Incompatible Polymer Combinations by Form Fit Using the Vibration Welding Process. *Int. J. Polym. Sci.* **2017**, *2017*, 6809469 doi:10.1155/2017/6809469. [[CrossRef](#)]
29. Mathijssen, D. Leading the way in thermoplastic composites. *Reinf. Plast.* **2016**, *60*, 405–407. [[CrossRef](#)]
30. André, N.M.; Goushegir, S.M.; dos Santos, J.F.; Canto, L.B.; Amancio-Filho, S.T. Friction Spot Joining of aluminum alloy 2024-T3 and carbon-fiber-reinforced poly(phenylene sulfide) laminate with additional PPS film interlayer: Microstructure, mechanical strength and failure mechanisms. *Compos. Part B Eng.* **2016**, *94*, 197–208. [[CrossRef](#)]
31. TenCate Advanced Composites BV. *Data Sheet: Cetex TC1100 PPS*; TenCate Advanced Composites BV: Morgan Hill, CA, USA, 2019. Available online: [https://www.toraytac.com/media/221a4fcf-6a4d-49f3-837f-9d85c3c34f74/smphpw/TAC/Documents/Data\\_sheets/Thermoplastic/UD%20tapes,%20prepregs%20and%20laminates/Toray-Cetex-TC1100\\_PPS\\_PDS.pdf](https://www.toraytac.com/media/221a4fcf-6a4d-49f3-837f-9d85c3c34f74/smphpw/TAC/Documents/Data_sheets/Thermoplastic/UD%20tapes,%20prepregs%20and%20laminates/Toray-Cetex-TC1100_PPS_PDS.pdf) (accessed on 14 March 2021).
32. Gemmel Metalle & Co. GmbH. *Technical Data Sheet: AlMgSi1 F30*; Gemmel Metalle & Co. GmbH: Berlin, Germany, 2019.
33. Meyer, S.P.; Wunderling, C.; Zaeh, M.F. Friction press joining of dissimilar materials: A novel concept to improve the joint strength. In Proceedings of the 22nd International ESAFORM Conference on Material Forming: ESAFORM 2019, Vitoria-Gasteiz, Spain, 8–10 May 2019; AIP Publishing: New York, NY, USA, 2019; p. 050031. [[CrossRef](#)]
34. Batz + Burgel GmbH & Co. KG. *Data Sheet: EN AW-2024*; Batz + Burgel GmbH & Co. KG: Friedberg, Germany, 2019.
35. Kumar, B.; Widener, C.; Jahn, A.; Tweedy, B.; Cope, D.; Lee, R. Review of the Applicability of FSW Processing to Aircraft Applications. In Proceedings of the 46th AIAA/ASME/ASCE/AHS/ASC Structures, Structural Dynamics and Materials Conference, Austin, TX, USA, 18–21 April 2005; American Institute of Aeronautics and Astronautics: Reston, VA, USA, 2005; p. 423. [[CrossRef](#)]
36. Lambiase, F.; Paoletti, A.; Grossi, V.; Di Ilio, A. Friction assisted joining of aluminum and PVC sheets. *J. Manuf. Process.* **2017**, *29*, 221–231. [[CrossRef](#)]
37. 3M. *Technical Data Sheet: Scotch-Weld Structural Plastic Adhesive: DP-8005*; 2020; Available online: <https://www.bindingsource.com/images/Custom-files/8005dsd.pdf> (accessed on 14 March 2021).
38. Oguma, H.; Naito, K. Effect of stress ratio on the fatigue fracture mechanism of adhesive single-lap joints: In case of GF/PP plates and an acrylic-based structural adhesive. *Procedia Struct. Integr.* **2019**, *19*, 224–230. [[CrossRef](#)]
39. DELO. *Data Sheet: DELO 02 Rapid*; 2020; Available online: [https://www.delo.de/fileadmin/datasheet/DELO-DUOPOX\\_02%20Rapid\\_%28TIDB-de%29.pdf](https://www.delo.de/fileadmin/datasheet/DELO-DUOPOX_02%20Rapid_%28TIDB-de%29.pdf) (accessed on 14 March 2021).
40. DELO. *Data Sheet: DELO-PUR AD948*; 2020; Available online: [https://substratec.com/de/download/1c1b1a18-66af-4eba-a4e6-fb9c5869f0de/DELO-PUR\\_AD948\\_%28TIDB-D%29.pdf](https://substratec.com/de/download/1c1b1a18-66af-4eba-a4e6-fb9c5869f0de/DELO-PUR_AD948_%28TIDB-D%29.pdf) (accessed on 14 March 2021).
41. Henkel AG. *Data Sheet: LOCTITE EA9466*; 2020; Available online: <http://tds.henkel.com/tds5/Studio/ShowPDF/EA%209466-EN?pid=EA%209466&format=MTR&subformat=REAC&language=EN&plant=WERCS> (accessed on 14 March 2021).
42. Spaggiari, A.; Dragoni, E. Effect of Mechanical Surface Treatment on the Static Strength of Adhesive Lap Joints. *J. Adhes.* **2013**, *89*, 677–696. [[CrossRef](#)]
43. Soykok, I.F. Degradation of single lap adhesively bonded composite joints due to hot water ageing. *J. Adhes.* **2017**, *93*, 357–374. [[CrossRef](#)]
44. Don, R.C.; Gillespie, J., Jr.; McKnight, S. Bonding Techniques for High Performance Thermoplastic Compositions. U.S. Patent 5643390A, 1 July 1997.
45. Soni, N.; Chandrashekar, S.; Kumar, A.; Chary, V. Defects Formation during Friction Stir Welding: A Review. *Int. J. Eng. Manag. Res.* **2017**, *7*, 121–125.
46. Ruhstorfer, M. Friction Stir Welding of Tubes. Ph.D. Thesis, Technical University of Munich (TUM), Munich, Germany, 2012.
47. *DIN 8580:2003-09, Manufacturing Processes—Terms and Definitions, Division*; Beuth Verlag GmbH: Berlin, Germany, 2003. [[CrossRef](#)]
48. *DIN 8593-0:2003-09, Manufacturing Processes Joining—Part 0: General: Classification, Subdivision, Terms and Definitions*; Beuth Verlag GmbH: Berlin, Germany, 2003. [[CrossRef](#)]
49. *DIN EN ISO 25239-1:2019-06, Friction Stir Welding—Aluminium—Part 1: Vocabulary*; Beuth Verlag GmbH: Berlin, Germany, 2019. [[CrossRef](#)]
50. *DIN 8593-6:2003-09, Manufacturing Processes Joining—Part 6: Joining by Welding*; Beuth Verlag GmbH: Berlin, Germany, 2003. [[CrossRef](#)]
51. *DIN 1910-100:2008-02, Welding and Allied Processes—Vocabulary—Part 100: Metal Welding Processes with Additions to DIN EN 14610:2005*; Beuth Verlag GmbH: Berlin, Germany, 2008. [[CrossRef](#)]
52. Liu, F.C.; Dong, P.; Lu, W.; Sun, K. On formation of Al O C bonds at aluminum/polyamide joint interface. *Appl. Surf. Sci.* **2019**, *466*, 202–209. [[CrossRef](#)]
53. *DIN 8593-8:2003-09, Manufacturing Processes Joining—Part 8: Joining by Means of Adhesives*; Beuth Verlag GmbH: Berlin, Germany, 2003. [[CrossRef](#)]
54. Otto Fuchs KG. *Technical Information: Material Data Sheet Aluminium*; Otto Fuchs KG: Meinerzhagen, Germany, 2019. Available online: <https://www.otto-fuchs.com/en/service/material-information.html> (accessed on 14 March 2021).